

Article

Simulation of Groundwater Flow and Migration of the Radioactive Cobalt-60 from LAMA Nuclear Facility-Iraq

Thair Sharif Khayyun

Building and Construction Engineering Department, University of Technology, Baghdad 35010, Iraq;
thshkhma@yahoo.com

Received: 30 June 2017; Accepted: 25 January 2018; Published: 9 February 2018

Abstract: This study provides a simulation of groundwater flow and advective-dispersive migration of radioactive Co-60 through an aquifer with three layers, which release or leak to groundwater from the Active Metallurgy Testing Laboratory (LAMA) Nuclear Facility-Iraq due to the nuclear accident scenario. Processing Modflow for windows (PMWIN) and Modular Three-Dimensional Multispecies Transport (MT3DMS) Models were used for this purpose. The study area and the contaminated area were 12.7 km² and 0.005625 km², respectively. Water levels of the groundwater have been measured in six monitoring wells. The simulation time was assumed to have started in 2016. The PMWIN model simulated the flow for two scenarios of water level in Tigris River (average and minimum water levels). The MT3DMS model simulated 10 years of plume travel, beginning in 2016. The simulated Co-60 concentrations after five years of travel were 32.34 and 34.44 µg/m³ for the two scenarios. The maximum predicted Co-60 concentrations at the end of Year 10 were 34.86 and 37.31 µg/m³, respectively. The sensitivity analysis showed that the simulated hydraulic heads in the observation wells and the simulated plume of Co-60 were highly sensitive to changes in the effective porosity but less sensitive to changes in other parameters of the dispersion and chemical reaction processes. The time necessary to reach steady state condition was predicted to be approximately 16 years. The contaminated area was isolated by using remedial process which is represented by three fully penetrating pumping wells with a suitable flow rate (0.045 m³/s) for controlling the movement of Co-60 pollutant.

Keywords: groundwater; pollutant; Co-60; LAMA Nuclear Facility

1. Introduction

It is important to estimate the concentration of the groundwater contamination under emergency conditions (release or leak of the radioactive materials due to nuclear accident scenario) and to estimate how the concentration of the contaminant will change with time and distance from the source of contamination. Iraq's industry has experienced a time of financial authorizes. This has prompted perpetual ecological issues, for example, releases of untreated effluent to surface waters, spillages and releases of chemicals to soils and groundwater. The current war has without a doubt exacerbated the constant ecological stresses that have collected in Iraq during recent decades. An essential part of the ecological harm related specifically with the war emerges from the plundering and looting of key frameworks and the stripping of supplies and equipment, including risky and radioactive materials. These industrial locales will posture critical dangers to human wellbeing and prompt further ecological corruption [1].

The AL-Tuwaitha Nuclear Research Center/Iraq were established in about 1960 and became the principle nuclear facility in Iraq. By 1991, the facility consisted of 90 buildings. It was heavily damaged by aerial bombings in 1991 and 2003. Research operations ceased in 1991 and the facility has been

used for storage since then [2]. Depending on the level of destruction, the remains of a particular building may consist of collapsed roofs, stand walls, exposed foundations, or piles of rubble and debris. Significant progress in the last few years has involved the characterization, decontamination and dismantlement of about 10 buildings including the LAMA (Active Metallurgy Testing Laboratory). Radioactively contaminated soil was present at 10 locations with elevated Uranium isotopes being the most common contaminant. Other elevated radionuclides were detected at four of the 10 sample locations, including Cesium-137, Strontium-90, Cobalt-60, Plutonium (238, 239 and 240) and various medical isotopes [3].

The ability to accurately predict the movement of contaminants through the groundwater flow system is an important element in the management and protection of groundwater resources. Numerical models can be developed to simulate the flow and the transport of groundwater solutes. Such models are useful for: (1) estimating the spatial and temporal variations in concentration of chemical constituents; (2) estimating the travel time of a contaminant from its source to the point of discharge; (3) aiding in the design of effective water quality monitoring systems; and (4) evaluating the feasibility and effectiveness of remedial procedures to remove contaminants from the aquifer or to prevent their spread [4]. The fate of transport of radionuclides stands out among the most imperative elements to be considered for the safety evaluation of repositories of radioactive wastes in permeable media. Research facility, Laboratory batch and column experiments were investigated to evaluate the transport of Cs-137 and Co-60 in loam and clay soils leached with groundwater using convection–dispersion equation model. The distribution coefficient (K_d) values for Cs-137 were found to be much higher as compared to Co-60. They ranged from 20 to 395 mL/g, depending on soil and radionuclide properties. The retardation factor (R) was 821 and 118 for Cs-137 while it was 65 and 88 for Co-60, for both soils, respectively. The dispersion coefficient (D) was 2.0 and 2.8 for Cs and 0.6 and 0.7 cm²/min for Co-60, respectively [5]. Three-dimensional numerical modeling is utilized to describe groundwater flow and contaminant transport at the nuclear test site in the center of north Nevada. Contaminants from the test are assumed to be all located within the cavity. Behaviors of the radionuclides are affected by the slow chemical release and retardation behavior. The transport calculations are sensitive to many flow and transport parameters. The impact of the porosity in radioactive decay is significant. For reactive solutes, retardation and the glass dissolution rate are also additionally basic [6]. The Nuclear Energy Institute (NEI (2007)) established a voluntary industry initiative for groundwater protection at nuclear power plants to improve utilities management and response to inadvertent release of radioactive materials in 2007. NEI commits each plant in the USA to implement the on-site groundwater protection program [7].

The aim of this study is to isolate the contaminated area with Co-60, utilizing fully penetrating pumping wells located next to the contaminated area. PMWIN model has to be developed for the LAMA Nuclear Facility-Iraq to calculate the required pumping rate of the wells. The pumping discharge must be sufficiently high so that the LAMA contaminated area with Co-60 lies within the capture zone of the pumping wells. The concentration distribution of the contaminant was computed after a simulation time.

2. Study Area

Figure 1 shows the Al-Tuwaitha Nuclear Research Center, which is located approximately 3 km south of the southern edge of Baghdad, Iraq, and approximately 0.8 km east of the Tigris River. Three research reactors were constructed at this site with 18 buildings. One of these buildings is the Active Metallurgy Testing Laboratory (LAMA). In 2002, IAEA conducted a hydro-geologic study that consisted of installing and sampling six groundwater monitoring wells [8]. The six wells range in depth from 12 to 42 m. Al-Tuwaitha is characterized by a hot, arid climate with intense sunshine for much of the year. The mean annual rainfall is 152 (mm). The potential evaporation rates are high exceeding 2000 mm in the summer.



Figure 1. Satellite image for Al-Tuwaittha Nuclear Research Center, Iraq.

3. Modeling of Groundwater Flow

3.1. The Governing Flow Equation

The flow rate of water through a porous media is related to the gradient of the hydraulic head, properties of water and the properties of the porous media as presented by Darcy's law:

$$q_i = -k_{ij} \frac{\partial h}{\partial x_j} \quad (1)$$

where q_i is the specific discharge in (m/s), k_{ij} is the hydraulic conductivity of the porous media in (m/s) and h is the hydraulic head in (m). A general form of the equation describing the transient flow in a nonhomogeneous anisotropic aquifer is derived by combining the continuity equation with Darcy's law. A general groundwater flow equation is:

$$\frac{\partial}{\partial x_j} \left(k_{ij} \frac{\partial h}{\partial x_j} \right) = S_s \frac{\partial h}{\partial t} + W \quad (2)$$

where S_s is the specific storage in m^{-1} , t is the time in s, W is the volumetric flux per unit volume in s^{-1} and x_j are the Cartesian coordinates.

The migration and mixing of chemicals dissolved in groundwater will be affected by the velocity of the flowing groundwater (specific discharge in Equation (1) represents the Darcy velocity and a volumetric flux per unit cross-sectional area). The actual seepage velocity (v_i) of groundwater for the actual cross-sectional area is as follows:

$$v_i = \frac{q_i}{n} \quad (3)$$

where n is the effective porosity of the porous media. Water in the ground moves orders of magnitude more slowly than it does in surface stream. The flow velocities of groundwater in gravel, fine sand and silty clay are 10^{-3} , 10^{-5} and 10^{-8} m/s, respectively [9].

3.2. The Transport of Contaminant

The transport of solutes in porous media, as in groundwater, can be described by three processes: advection (process of transfer of fluid through a geologic formation in response to a pressure gradient); hydrodynamic dispersion; and physical, chemical or biochemical reactions. The method of characteristics (MOC) is used to simulate the advection transport (the contaminants are represented by

several particles that move with the groundwater). The transport and dispersion of contaminant in flowing groundwater is derived from the principle of conservation of mass [10]. A general form of the solute-transport equation is as follows [11]:

$$\frac{\partial(nC)}{\partial t} = \frac{\partial}{\partial x_i} (nD_{ij} \frac{\partial C}{\partial x_j}) - \frac{\partial}{\partial x_i} (ncv_i) - c^*W + chem \quad (4)$$

$$\begin{aligned} chem &= -\rho_b \frac{\partial C^-}{\partial t} && \text{for linear equilibrium controlled sorption} \\ &= \sum R_k && \text{for chemical rate-controlled} \\ &= -\delta(nC + \rho_b C^-) && \text{for decay} \end{aligned}$$

where D_{ij} is the coefficient of hydrodynamic dispersion (m^2/s), c^* is the concentration of the solute in the fluid, C^- is the concentration of the species adsorbed on the solid, ρ_b is the bulk density of the sediment (kg/m^3), R_k is the rate of production of the solute in reaction K ($kg/(m^3 \cdot s)$) and δ is the decay constant (s^{-1}) [12]. The first term on the right side of Equation (4) represents the change in concentration due to hydrodynamic dispersion. The dispersive flux occurs in a direction from higher toward lower concentrations (Fick's law). The coefficient of dispersion (D_{ij}) is characterized as the total of mechanical dispersion (porous medium and fluid flow) and molecular diffusion [10].

The equation of coefficient of dispersion is given as:

$$D_{ij} = \alpha_{ijmn} \frac{V_m V_n}{|V|} + D_m \quad (5)$$

where α_{ijmn} is the dispersivity of the porous medium (m); V_m and V_n are the component of the velocity of the fluid flow in the m and n directions, respectively (m/s); D_m is the coefficient of molecular diffusion (m^2/s) and $|V|$ is the velocity vector [13]. The dispersivity can be defined by the longitudinal dispersivity α_L and the transverse dispersivity α_T . These are related to the longitudinal and transverse dispersion coefficients by $D_L = \alpha_L |V|$ and $D_T = \alpha_T |V|$. It is found that α_L is proportional to the measurement scale. Its value is in a range from 0.01 to 1.0 times the scale of the measurement. For unconsolidated media (sand), the dispersivity in the direction of flow is as follows [14]:

$$\alpha_L = 0.2 L^{0.44} \quad (6)$$

where L is the flow distance (path). Transverse dispersivity is generally smaller than longitudinal dispersivity ($\alpha_T = (0.01 \text{ to } 0.10) \alpha_L$).

The types of reactions are affected by:

1. First order rate reaction (radioactive decay).
2. Retardation factor (sorption-desorption reaction governed by a linear isotherm and constant distribution coefficient (K_d)).

The common method of estimating contaminant retardation is based on the partition coefficient (constant distribution coefficient) (mL/g), which is defined as the ratio of the quantity of the adsorbate adsorbed per mass of solid to the amount of the adsorbate remaining in solution at equilibrium. The values of constant distribution coefficient for Co-60 vary between 2.23 and 52.5 mL/g for all media [15]. The chemical retardation is defined as the ratio of the velocity of the water through a control volume to the velocity of the contaminated water. Its value is greater than 1 due to solute sorption to soils. For porous flow with saturated moisture conditions, the retardation factor R_f is defined as:

$$R_f = 1 + \left(\frac{\rho}{n} \right) k_d \quad (7)$$

where ρ the bulk density (kg/m^3) and n is effective porosity. The retardation factor values (R) for Co-60 vary between 65 and 88 and the dispersion coefficient was $0.6\text{--}0.7 \text{ cm}^2/\text{min}$.

3.3. Groundwater Numerical Model

In this study, PMWIN model was utilized. It is a three-dimensional finite differences groundwater model. The uses of this model are to run a steady state flow simulation, calculate water budget, and simulate solute transport by using the method of characteristics solution and first order Euler particle tracking algorithm and parameter estimation (finding a set of parameters or boundary conditions so that the simulated values match the measured values to a sensible degree).

4. Methodology

4.1. Groundwater Flow Modeling

A groundwater flow modeling has been applied for an area of $2925 \text{ m} \times 4350 \text{ m}$ of the Al-Tuwaith site in Baghdad, with a grid interval of 75 m. According to previous studies, the hydrogeological cross-sections show that there are three layers of soils (light brown clay, grey silt to fine sand and grey medium sand) (Figure 2). The thickness of these layers is 16 m, 10 m and 24 m, respectively. The average elevation of the ground surface is 31.20 (m.a.s.l.). It represents the top of the first layer. The average groundwater levels monitored by [2,16] for each of the monitoring wells and for the dry and wet (raining) seasons in 2011 and 2002 are summarized in Table 1. The direction and the water levels of groundwater in Baghdad City are shown in Figure 3, [17]. The aquifer system of the study area is unconfined. The west side is bounded by the Tigris River and the east side can be considered as a fixed head boundary. The Tigris River had a high, an average and low water stage of 30.70, 29.15 and 27.60 m.a.s.l., respectively, for the period 2000–2015, [18].

Table 1. Variation of groundwater level for wells, m.a.s.l. (2002 and 2011).

Year	Well No.					
	1	2	3	4	5	6
Dry season 2011	26.20	26.00	26.25	26.50	25.70	26.60
Wet season 2011	26.90	26.70	26.83	27.10	26.24	27.10
2002	27.80	27.70	27.60	27.81	28.05	27.85
Average	26.97	26.8	26.89	27.14	26.66	27.18

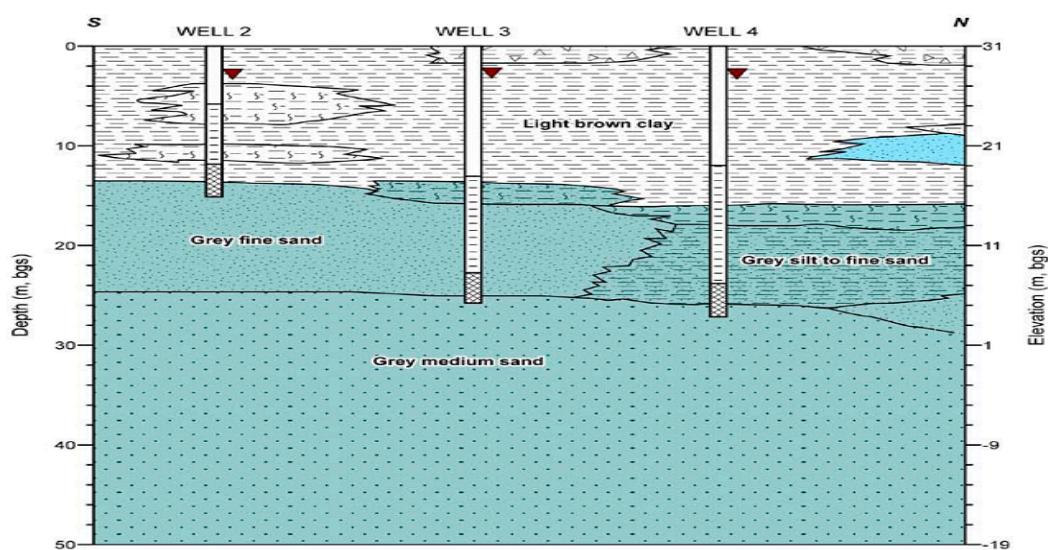


Figure 2. Hydrogeological cross-section of the study area.

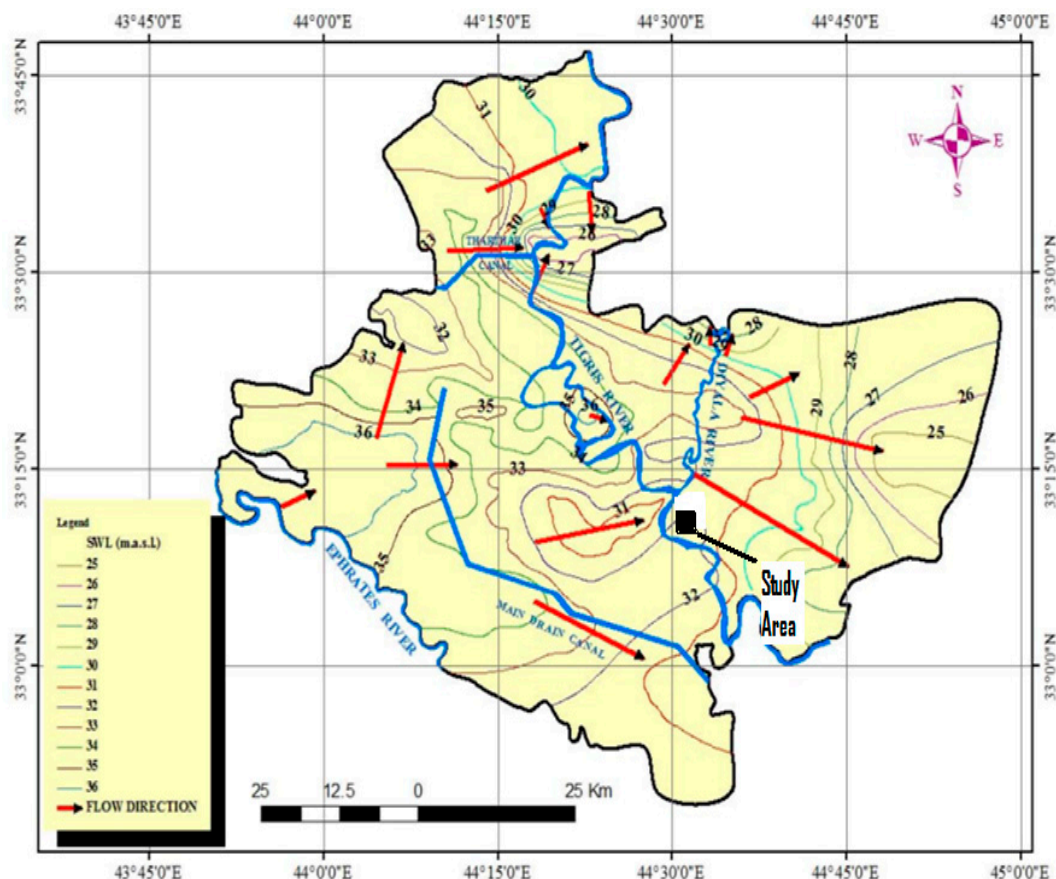


Figure 3. The directions and water levels of groundwater flow, Baghdad city.

The initial condition was specified with the elevation of water table equal to 25.50 (m.a.s.l.). The horizontal hydraulic conductivities, bulk densities and the effective porosities of the soils, which match the properties of the three layers, are summarized in Table 2, [13]: The vertical hydraulic conductivity is assumed to be 10% of the horizontal hydraulic conductivity. A constant recharge rate of $(2.19 \times 10^{-5} \text{ m/day})$ was applied to the aquifer [19]: The contaminated area, which was 0.005625 km^2 , lies in the first layer next to the east boundary (Figure 1). Fully penetrating wells were used which were located next to the eastern boundary of the study area. A numerical model (PMWIN) was used to calculate the required pumping discharge of these wells and PMpath model was used to compute the capture zone of the pumping wells.

Table 2. Soil properties of the three layers.

Layer	Depth m	Soil	$K_H \text{ cm/s}$	Bulk Density kg/m^3	Effective Porosity %
1	16	Light brown clay	10^{-8} – 10^{-5}	1200–1500	1–18
2	10	Grey silt to fine sand	10^{-5} – 10^{-3}	1400–1600	1–39
3	24	Grey medium sand	10^{-3} – 10^{-1}	1600–1700	16–46

4.2. Cobalt-60 Transport

In this study, MT3D model was used to simulate the contaminant transport of Co-60. This simulation was based on the calculated groundwater flow field. The guidance values for radioactivity in drinking water were recommended [20]. The SI unit of radioactivity is the Becquerel (Bq), where $1 \text{ Bq} = 1 \text{ disintegration per second}$. Guidance levels for drinking water are given as the activity of the radionuclide per liter, called the activity concentration (Bq/L). The radiation

dose resulting from ingestion of radionuclide depends on several chemical and biological factors. The guidance level for Co-60 in drinking water is 100 Bq/L. Risk-based criteria for primary radionuclides (Co-60) in water is less than $1.2 \times 10^{-4} \mu\text{g}/\text{m}^3$ and in soils varies widely, ranging from 1 to 40 ppm by weight. These levels apply to radionuclides released due to nuclear accidents that have occurred before. One gram of Co-60 has an activity of 44 TBq. The estimated volume of radioactive waste at LAMA site in Iraq was about 1.0 metric tonne [21]. Due to the constant recharge rate of $2.19 \times 10^{-5} \text{ m/day}$ which is applied to the aquifer, the calculated dissolved rate of the Co-60 into groundwater was $0.6 \times 10^{-6} \mu\text{g}/\text{s}/\text{m}^2$. The calculated longitudinal and transverse dispersivities of the study area aquifer are $\alpha_L = 5.0 \text{ m}$ and $\alpha_T = 0.05\text{--}0.5$, respectively, according to Equation (6). For this study, the transverse dispersivity (α_T) is assumed to be 10% of the longitudinal dispersivity. The flow path was about 1200 m. The retardation factor is calculated by using Equation (7), and the initial concentration molecular diffusion coefficient is assumed to be $1 \times 10^{-8} \text{ m}^2/\text{s}$ (approximately equal to zero). In this study, the initial condition was specified with Co-60 concentration equals 0 mg/L. The concentration distribution will be calculated after simulation time of 10 years and the relationship between the concentrations of Co-60 versus time at many points in the mesh of the study area was displayed.

5. Results of Modeling

5.1. Groundwater Flow Modeling

The groundwater flow in the 12.70 km^2 of the study area was analyzed by using two scenarios of water surface elevation in Tigris River (29.20 m.a.s.l. (Scenario 1) and 27.60 m.a.s.l. (Scenario 2), respectively). The contaminated area was isolated by using three fully penetrating wells located next to the southeast of the boundary. This position depends on the direction of the flow path of the groundwater from (NW-SE). The total distance between them was approximately 215 m. As the first layer is unconfined for the study area, it is difficult to know the saturated thickness and the transmissivity of this layer and to know the pumping rate for each layer. The U.S. Geological Survey, in cooperation with the Minnesota Department of Natural Resources, conducted a study to characterize ground-water flow conditions surrounding aquifers. Average hydraulic conductivity values ranged from 0.05 to 5.0 ft/day for sands and clays and from 0.01 to 121 ft/day for coarse sands, gravels, and boulders. The simulated net ground-water flow was $+1.34 \text{ ft}^3/\text{s}$ ($0.036 \text{ m}^3/\text{s}$), and the net groundwater flow calculated was $+5.4 \text{ ft}^3/\text{s}$ ($0.146 \text{ m}^3/\text{s}$). Simulated water levels and groundwater flow for the calibrated steady-state simulation were most sensitive to changes in horizontal hydraulic conductivity, suggesting that this characteristic is the predominant parameter controlling steady-state water-level and flow conditions [22]. Thus, by using a trial and error method and the properties of the aquifer, the pumping rate for each pump was $0.015 \text{ m}^3/\text{s}$ so that the contaminated area lies within the capture zone of the pumping wells. PMWIN-PRO and PMPATH were used to construct the numerical model and to compute the capture zone of the pumping wells. The properties of the aquifer values were adjusted until simulated groundwater level in the wells matched those observed in 2002 and 2011. The steps followed to reach the calibration of the model were by using an initial estimate of the hydraulic conductivity and effective porosity. A solution computed with this initial model will then be imported and the error in the initial solution will be analyzed, New values for hydraulic conductivity and effective porosity will then be entered and a new solution will be generated and a new error estimate will be computed. These steps will be repeated until the error is reasonably small. The best match was achieved with an aquifer horizontal hydraulic conductivity for the three layers of (5×10^{-7} , 5×10^{-4} , and $3 \times 10^{-2} \text{ cm/s}$, respectively). The effective porosity values were 16%, 28% and 35%, respectively (Table 3). The flow, plume extent velocity, dispersion coefficient and retardation were highly sensitive to change in the effective porosity. The simulated flow and equipotential lines of the groundwater for the two scenarios are shown in Figures 4–7. The simulated water table elevation near the three pumping wells was 20.96 m.a.s.l.

Table 3. Calibration of the Processing Modflow model parameters.

Layer	Soil	Hydraulic Conductivity		Effective Porosity	
		Default Value cm/s	Calibrated Value cm/s	Default Value %	Calibrated Value %
1	Light brown clay	10^{-8} – 10^{-5}	5×10^{-7}	1–18	16
2	Grey silt to fine sand	10^{-5} – 10^{-3}	1×10^{-4}	1–39	28
4	Grey medium sand	10^{-3} – 10^{-1}	3×10^{-2}	16–46	35

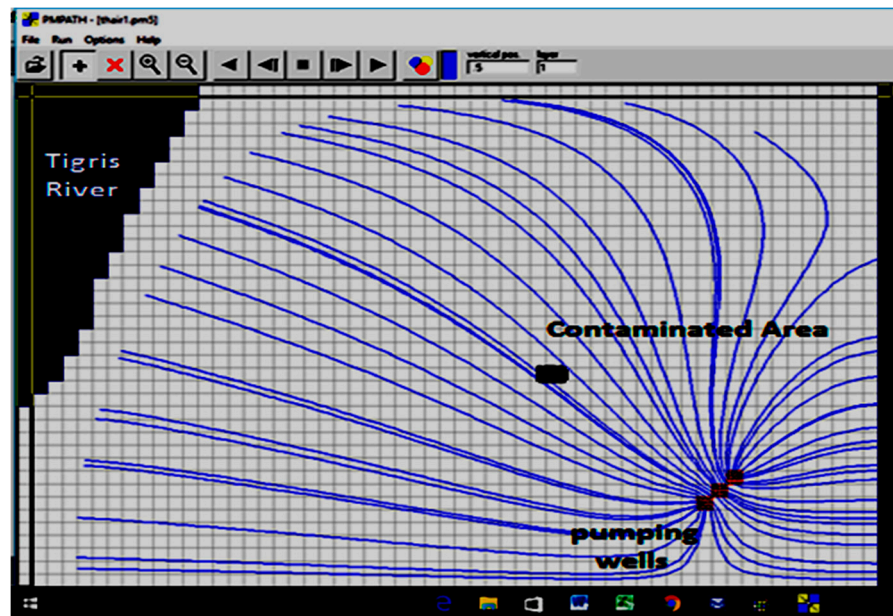


Figure 4. Groundwater flow directions for Scenario 2.

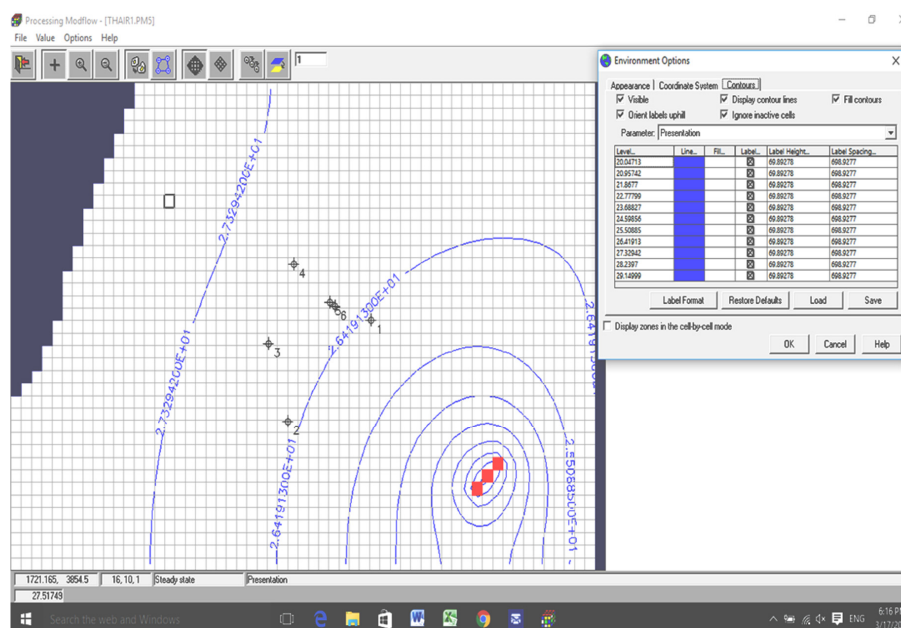


Figure 5. Groundwater equipotential contour lines for Scenario 2.

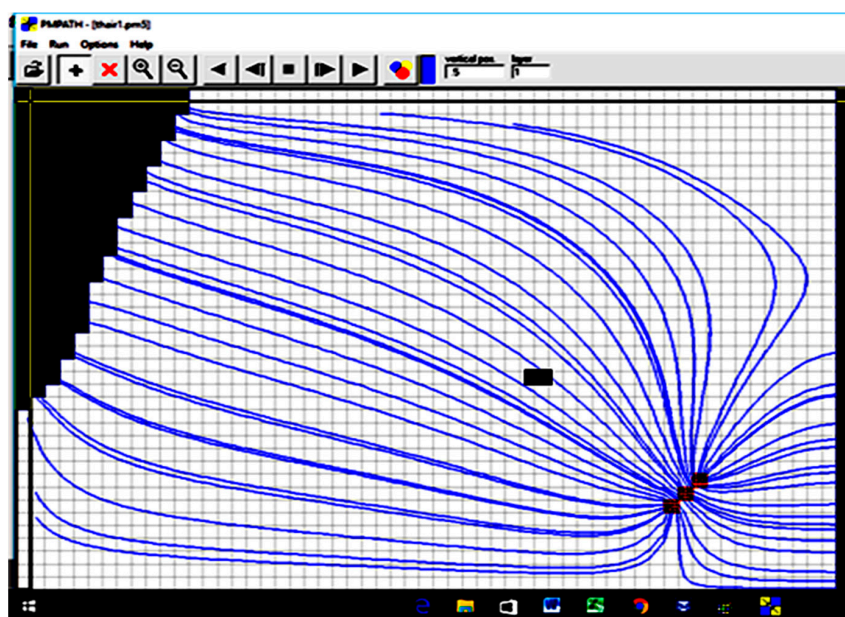


Figure 6. Groundwater flow directions for Scenario 1.

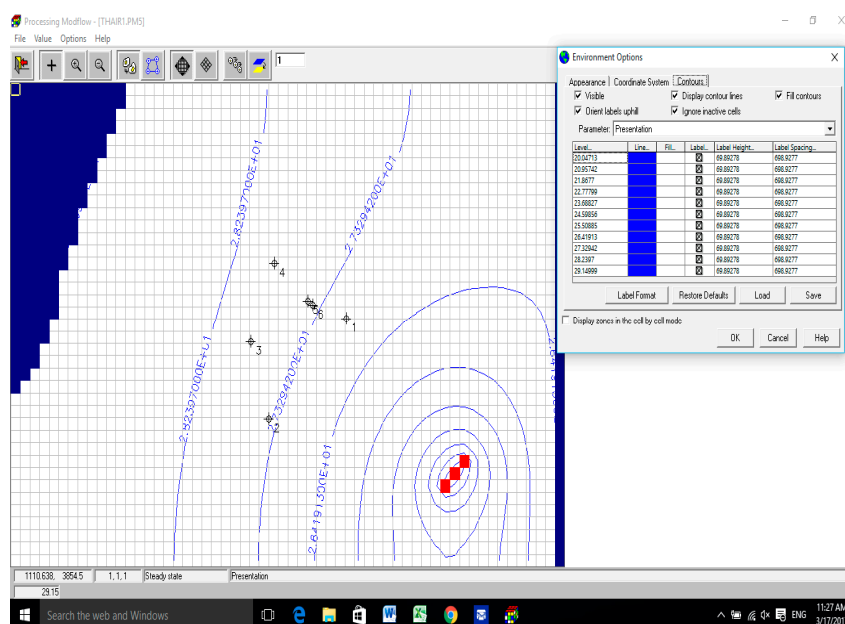


Figure 7. Groundwater equipotential contour lines for Scenario 1.

The results of the calibration of flow model is accomplished by scatter diagrams (Figures 8 and 9) for the two scenarios which represent the observed groundwater surface elevations of the wells (average value of the groundwater level through the years 2002 and 2011) against the corresponding simulated values. There is a good agreement between them for each scenario. The existence of large area of scatter around a 45° line is due to the differences in time of water surface measurements of Tigris River and the differences between the input data of the model boundary condition and the water levels monitored in 2002 and 2011. The match between the simulated and observed groundwater elevation indicates that the model can be considered calibrated and it can be used for the plume migration of Co-60 contaminant.

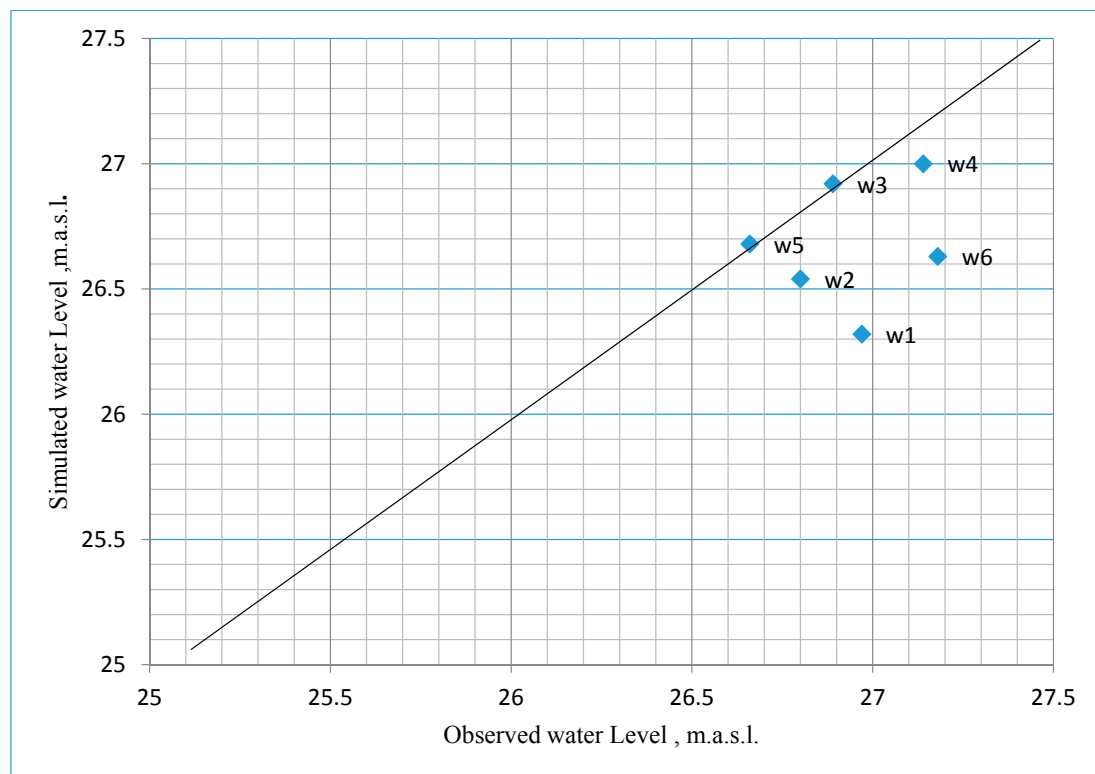


Figure 8. Comparison of simulated and observed heads for minimum water surface elevation of Tigris River (27.60 m.a.s.l.), Scenario 2.

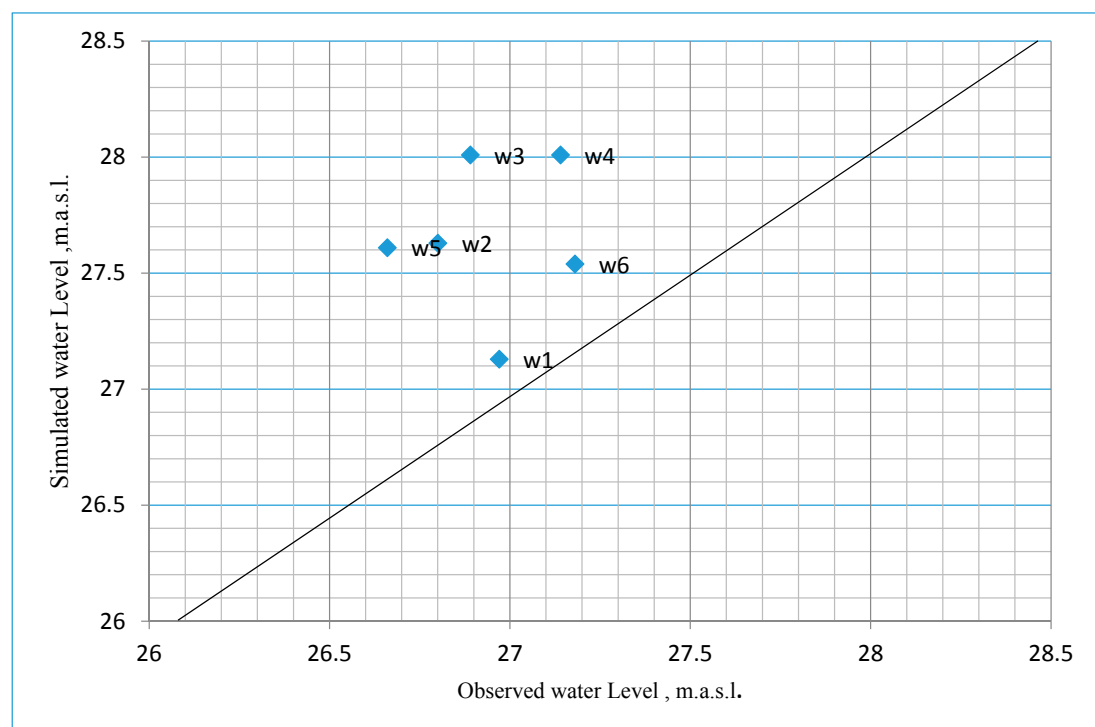


Figure 9. Comparison of simulated and observed heads for average water surface elevation of Tigris River (29.20 m.a.s.l.), Scenario 1.

5.2. Co-60 Transport Modeling

Plume migration of Co-60 from LAMA Nuclear Facility area was simulated over a 10-year period using MT3DMS model. MOC method and first order Euler were selected for the solution scheme and for the particle tracking algorithm, respectively. At the start of the simulation, the initial concentration value of Co-60 was zero $\mu\text{g}/\text{m}^3$ throughout the study area. The used value of Co-60 concentration in the simulation was $2367 \mu\text{g}/\text{m}^3$ and it distributed uniformly along the contaminated area (5625 m^2). The ratio of longitudinal to transverse dispersivity was 10:1. This study used a value of $0.01 \text{ m}^3/\text{kg}$ for the distribution coefficient of the Co-60 in the porous media so the average retardation factor value was 70. The time of simulation was one year (2016). The time step was $1.4334 \times 10^7 \text{ s}$, thus for a five-year period, there are 11 times steps. Figures 10–13 show the extent of Co-60 pollutant concentrations from the LAMA area after 5 and 10 years for the two scenarios. Contour lines of equal Co-60 concentration were plotted as a result of the simulations of the transport of the contaminant at the end of Year 5 and Year 10 and for both scenarios. The $4.32 \mu\text{g}/\text{m}^3$ contour is used to delineate the extent of the Co-60 plume. The simulated extents of the Co-60 plume from the start of 2016 through the end of 2020 and 2021 through the end of 2025 were illustrated in these figures. It is difficult to make a model calibration for the transport of Co-60 since the monitoring wells positions were outside the direction of flow from the LAMA area to the three pumping wells. Furthermore, no water quality data exist for Co-60 concentrations. After 5 and 10 years, the plume extends 450–700 m for Scenario 2 and 860–1000 m for Scenario 1 with an average width of 260 m. The maximum predicted Co-60 concentration at the end of Years 5 and 10 were $32.34\text{--}34.44 \mu\text{g}/\text{m}^3$ and $34.86\text{--}37.31 \mu\text{g}/\text{m}^3$, respectively. The extent of plume after 10 years reaches the position of the three pumping wells.

The maximum Co-60 concentrations in the study area were approximately the same in both scenarios. The average flow velocity of the groundwater was approximately $3.2 \times 10^{-6} \text{ m/s}$. The MODFLOW model (PMWIN and MT3DMS) was run at steady state condition and for a long time. The plume of Co-60 contaminant after a 16-year period approximately match the plume of the steady state condition.

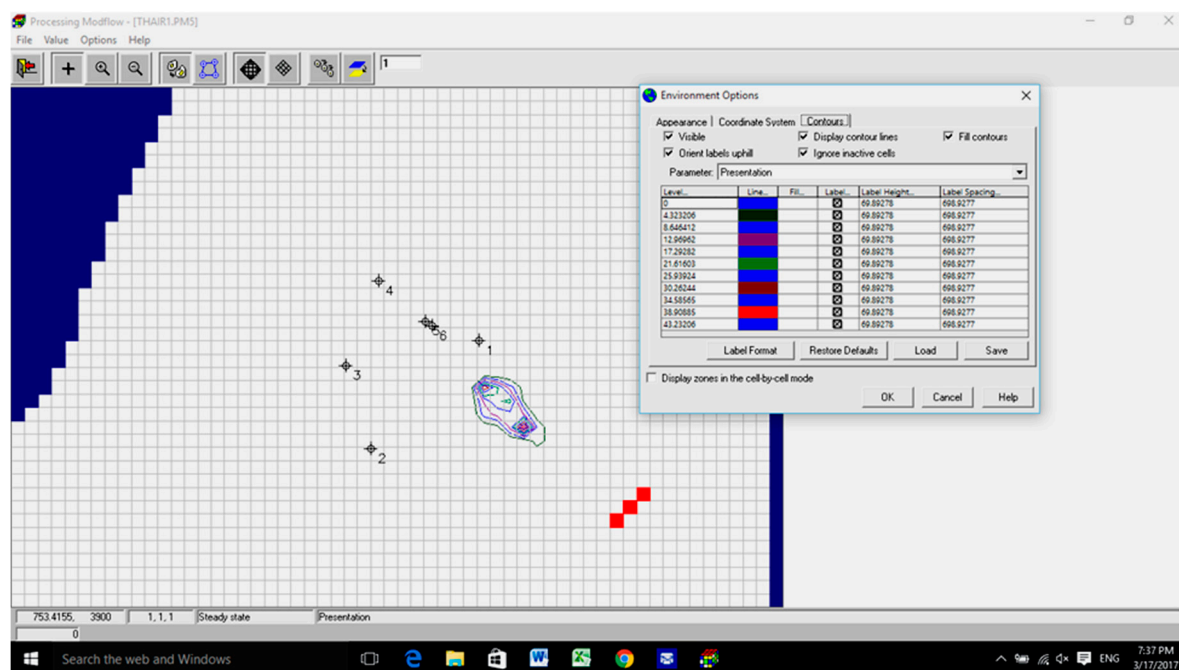


Figure 10. The extent of Co-60 pollutant concentrations from the LAMA area after five years for Scenario 2.

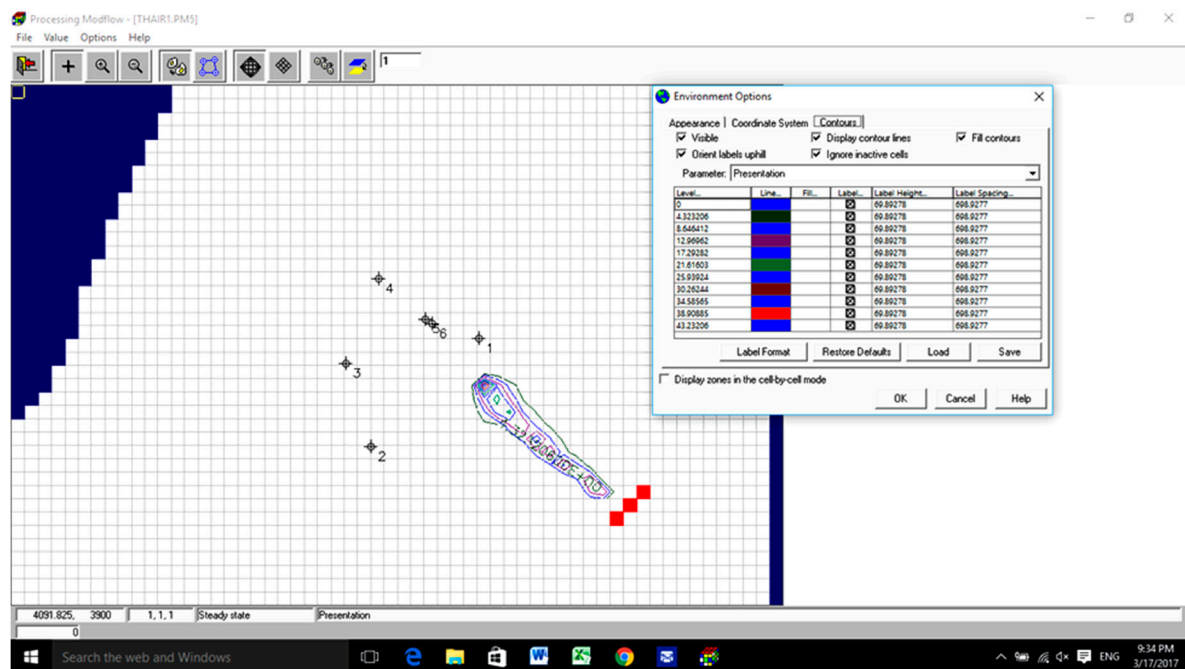


Figure 11. The extent of Co-60 pollutant concentrations from the LAMA area after 10 years for Scenario 2.

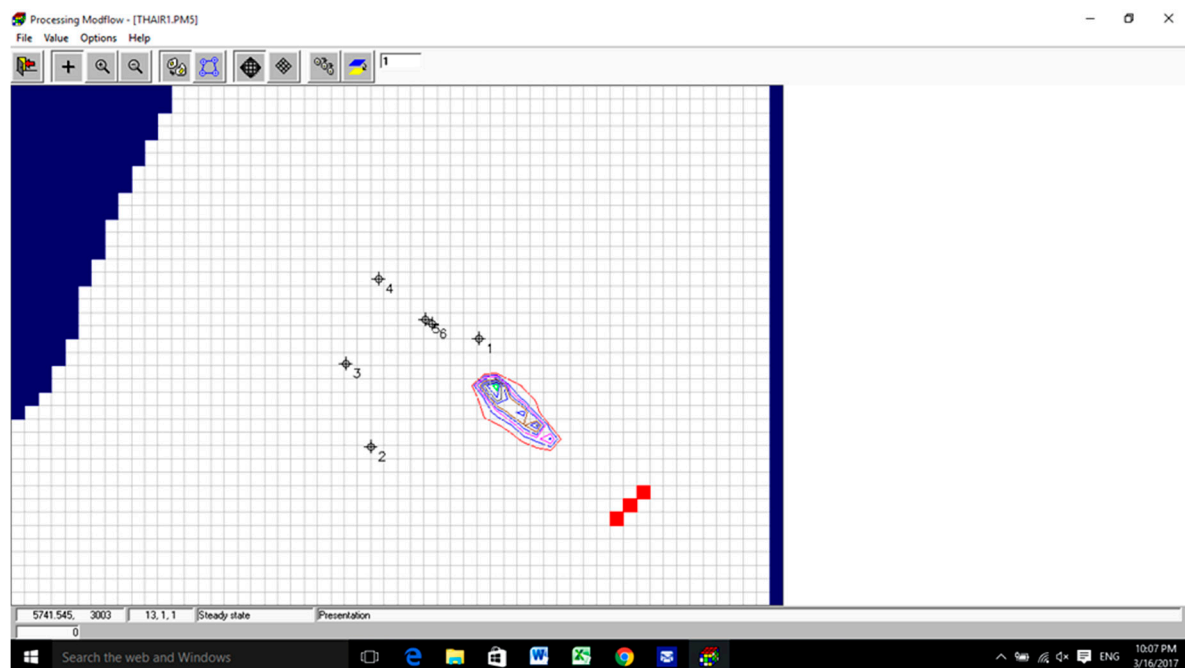


Figure 12. The extent of Co-60 pollutant concentrations from the LAMA area after five years for Scenario 1.

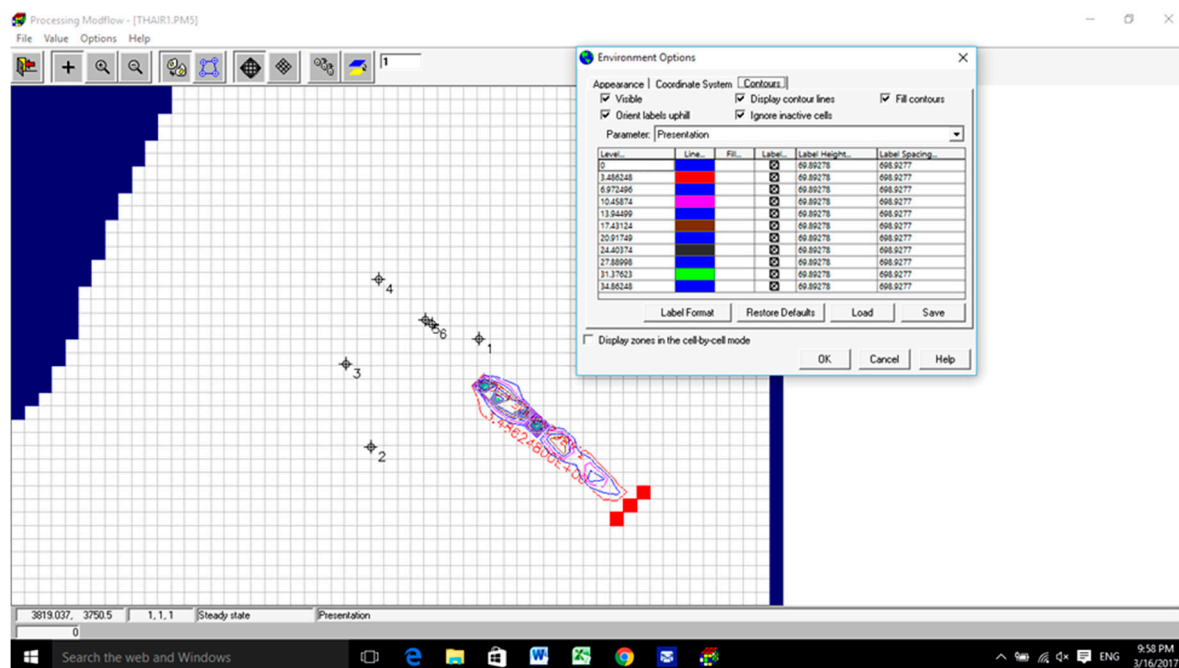


Figure 13. The extent of Co-60 pollutant concentrations from the LAMA area after 10 years for Scenario 1.

6. Conclusions

The results of this study indicate that the model PMWIN and MT3DMS can be used to simulate the groundwater flow and solute transport of Co-60 under different conditions, although the model calibration has some difficulties for many variables of the advective, dispersion and chemical reactions. The direction of groundwater flow in this study matches with the results presented as in [17], (Figure 3), who prepared a map for the groundwater elevations in Baghdad. Three wells with discharging pumps were placed perpendicular to the Co-60 plume or to the direction of flow. The total pumping rate was $0.045 \text{ m}^3/\text{s}$ ($0.015 \text{ m}^3/\text{s}$ for each pump). These pumps were used to recover the Co-60 pollutant. A treatment plant will be placed close to the pumps position to treat the pumped water after 10 years. These pumps and their locations are suitable for remediating the contamination of water with Co-60. The pump and treatment method may be considered expensive, thus, for contaminated water to be remediated, a permeable reactive barrier with suitable material can be used as an alternative solution for removing Co-60 pollutant. The velocity of groundwater flow in this study was $3.2 \times 10^{-6} \text{ m/s}$. It is an acceptable value but it can be checked by using aquifer testing data because literature for this site is not available. Many observation wells must be constructed in the study area, positioned between the LAMA Nuclear Facility and the pumping well for recovery of the contaminant water. The results of the maximum concentration of Co-60 contaminant show that the transport of the pollutants is slow relative to the velocity of the water in the aquifer. This slow movement is due to sorption and high retardation factor of the Co-60 which depends on the partition coefficient. The maximum predicted Co-60 concentration at the end of Year 10 was $37.31 \mu\text{g}/\text{m}^3$.

Conflicts of Interest: The author declares no conflict of interest.

References

1. UNEP (United Nations Environment Program). *Environmental in Iraq: UNEP Progress Report*; United Nation Environment Program: Geneva, Switzerland, 2003.
2. Sandia National Laboratories. *Groundwater Monitoring Program Plan and Conceptual Site Model for Al-Tuwaittha Nuclear Research Center in Iraq*; Sandia Report; Sandia National Laboratories: Livermore, CA, USA, 2013.

3. IAEA (Iraq Atomic Energy Commissio). *Piecing Together Iraq's Nuclear Legacy*; Bulletin of the Atomic Scientists: Chicago, IL, USA, 1991.
4. Eliezer, J.W. *Groundwater Flow and Solute Transport at a Municipal Landfill Site on Long Island*; Water Resources Investigations Report, 86-4207; U.S. Geological Survey: New York, NY, USA, 1988.
5. Ramzi, M. Shihab Modeling of Cs-137 and Co-60 Transport in Calcareous Soils by Groundwater. *J. Soil Sci. Environ. Manag.* **2014**, *5*, 52–61.
6. Grey, P.; Ahmed, E. *Modeling Groundwater Flow and Radioactive Transport in a Fractured Aquifer*; Water Resources Center: Las Vegas, NV, USA, 1999; Volume 37.
7. NEI (Nuclear Energy Institute). *Industry Groundwater Protection Initiative*; Final Guidance Document; Nuclear Energy Institute: Washington, DC, USA, 2007.
8. Abbas, M.J.; Latif, K.H.; Ahmed, B.A. *Groundwater Monitoring Program at AL-Tuwaittha Nuclear Research Center, Iraq*; Informal Paper; National Nuclear Security Administration: Washington, DC, USA, 2010; p. 21.
9. Peter, W. *A Non-Technical Guide to Groundwater Modeling*; U.S. Department of Energy Hanford Site: Washington, DC, USA, 2007.
10. Bear, J. *Hydraulics of Groundwater*; McGraw-Hill: New York, NY, USA, 1979; p. 569.
11. Jacques, W. *The Handbook of Groundwater Engineering*; School of Civil Engineering, Purdue University: West Lafayette, IN, USA, 1999.
12. Grove, D.B. *Derivation of Equations Describing Solute Transport in Groundwater*; U.S. Geological Survey, Water Resources Investigations: New York, NY, USA, 1976.
13. Domenico, P.A.; Schwartz, F.W. *Physical and Chemical Hydrogeology*; John Wiley and Sons: New York, NY, USA, 1990; p. 709.
14. Schulze-Makuch, D. Longitudinal Dispersivity Data and Implications for Scaling Behavior. *Groundwater* **2005**, *43*, 443–456. [[CrossRef](#)] [[PubMed](#)]
15. Larry, M.; Terry, S. *Sorption K_d Measurements on Cinder Block and Grout in Support of Dose Assessments for Zion Nuclear Station Decommissioning*; Informal Report; Environmental and Climate Sciences Department, Brookhaven National Laboratory: New York, NY, USA, 2014.
16. Naseer, H. Evaluation of the Groundwater in Baghdad Governorate-Iraq. *J. Sci.* **2015**, *56*, 1708–1718.
17. Al-Adili, A.; Ali, S. Hydro-Chemical Evolution of Shallow Groundwater System within Baghdad City-Iraq. In *Proceedings of the Tenth International Water Technology Conference (IWTC10 2006)*, Alexandria, Egypt, 23–25 March 2006; pp. 23–25.
18. Ministry of Water Resources—Iraq. *Flow Rates of Water in Tigris River*; Report; National Center for Water Resources Management: Baghdad, Iraq, 2015.
19. Bashoo, D.; Lazim, S.; Alwan, M. *Hydrogeology of Baghdad Province*; Internal Report; General Directorate of Water Well Drilling: Baghdad, Iraq, 2005.
20. ICRP (International Commission on Radiological Protection). *Guidelines for Drinking Water Quality*; World Health Organization: Geneva, Switzerland, 1991.
21. Al-Musawi, F. *Radioactive Waste Management Policy and Strategy in Iraq*; Deputy Minister, Ministry for Science and Technology: Baghdad, Iraq, 2010; p. 24.
22. Perry, M.J. *Characterization of Groundwater Flow Surrounding Aquifers*; Water Resources Investigations Report, 02-4198; U.S. Geological Survey: Mound View, MN, USA, 2002; p. 24.



© 2018 by the author. Licensee MDPI, Basel, Switzerland. This article is an open access article distributed under the terms and conditions of the Creative Commons Attribution (CC BY) license (<http://creativecommons.org/licenses/by/4.0/>).